Implanted adipose progenitor cells as physicochemical regulators of breast cancer

Emily M. Chandler[a,1], Bo Ri Seo[a,1], Joseph P. Califano[a], Roberto C. Andresen Eguiluz[b], Jason S. Lee[a], Christine J. Yoon[a], David T. Tims[a], James X. Wang[a], Le Cheng[c], Sunish Mohanan[c], Mark R. Buckley[d], Itai Cohen[d], Alexander Yu Nikitin[c], Rebecca M. Williams[a], Delphine Gourdon[b], Cynthia A. Reinhart-King[a], and Claudia Fischbach[a,2]

[a]Department of Biomedical Engineering, Cornell University, Ithaca, NY 14853; [b]Department of Materials Science and Engineering, Cornell University, Ithaca, NY 14853; [c]Department of Biomedical Sciences, Cornell University, Ithaca, NY 14853; and [d]Department of Physics, Cornell University, Ithaca, NY 14853

Edited by* Robert Langer, MIT, Cambridge, MA, and approved May 4, 2012 (received for review January 2, 2012)

Multipotent adipose-derived stem cells (ASCs) are increasingly used for regenerative purposes such as soft tissue reconstruction following mastectomy; however, the ability of tumors to commandeer ASC functions to advance tumor progression is not well understood. Through the integration of physical sciences and oncology approaches we investigated the capability of tumor-derived chemical and mechanical cues to enhance ASC-mediated contributions to tumor stroma formation. Our results indicate that soluble factors from breast cancer cells inhibit adipogenic differentiation while increasing proliferation, proangiogenic factor secretion, and myofibroblastic differentiation of ASCs. This altered ASC phenotype led to varied extracellular matrix (ECM) deposition and contraction thereby enhancing tissue stiffness, a characteristic feature of breast tumors. Increased stiffness, in turn, facilitated changes in ASC behavior similar to those observed with tumor-derived chemical cues. Orthotopic mouse studies further confirmed the pathological relevance of ASCs in tumor progression and stiffness in vivo. In summary, altered ASC behavior can promote tumorigenesis and, thus, their implementation for regenerative therapy should be carefully considered in patients previously treated for cancer.

mechanobiology | desmoplasia | angiogenesis | tissue engineering

ASCs are widely used in tissue engineering due to their multipotency, ability to enhance vascularization, and relative ease of isolation from the stromal vascular fraction of adipose tissue (1, 2). In particular, ASCs are increasingly considered for reconstructive procedures following surgery for breast cancer, which compose the majority of the 93,000 breast reconstructions performed in the United States per year (3). ASCs offer several advantages over commonly utilized silicone and saline implants including their ability to regenerate functional adipose tissue, which reconstitutes a large fraction of the breast (4, 5); however, malignantly transformed cells may be present in breast cancer survivors without manifest disease, and it remains unclear whether implanted ASCs may increase the risk of tumor development and relapse (6) by establishing a microenvironment conducive to nascent or recurrent tumorigenesis.

Mammary tumors are stiffer than normal mammary gland tissue (7, 8), due in part to tumor-cell secreted morphogens that vary ECM assembly. Altered ECM deposition and contraction not only enhances tumor rigidity (9) but further modulates tumor progression by perturbing epithelial morphogenesis (10) and vascular development (11). Myofibroblasts regulate these outcomes by controlling the mechanical properties of the tumor-associated ECM and by functioning as a major source of host-derived proangiogenic factors (e.g., VEGF) (9, 12). Generally, local fibroblasts are considered the primary origin of myofibroblasts and regulator of this desmoplastic reaction, but bone marrow-and tissue-derived mesenchymal stem cells may also contribute to this cell population. Specifically, approximately 20% of tumor-associated α-smooth muscle actin (α-SMA) positive myofibroblasts originate from bone marrow, whereas nonbone marrow tissues including adipose tissue contribute to the remainder (13, 14); however, the integrated effects of tumor-associated physicochemical cues on ASC-dependent tumorigenesis are not well understood.

Here, we applied a physical sciences-based approach to correlate tumor-mediated changes in ASC phenotype with tissue stiffness, vascularization, and growth. Our findings support that ASCs can develop into myofibroblasts in response to physicochemical factors provided by cancerous cells. This phenotypic change not only enhanced angiogenesis but also ECM rigidity, which further increased the tumor-promoting capacity of ASCs in a positive feedback loop. These findings support the role of ASCs as key regulators of mammary tumor progression and recurrence, which warrant review of current tissue engineering therapies following mastectomy and may be explored towards more efficacious therapies for breast cancer patients.

Results and Discussion

Tumor-Secreted Soluble Factors Regulate the Adipogenic and Proangiogenic Capability of ASCs. To evaluate the effects of tumor cell-secreted soluble factors on ASC behavior, human ASCs were cultured in tumor-conditioned media (TCM) from commonly used highly (MDA-MB231) or less (MCF-7) aggressive human breast cancer cell lines. Additionally, mouse 3T3-L1 preadipocytes-a well-characterized cell model for studies of adipogenesis (15)-were used to verify the broad implications from primary ASC studies. Analysis of cell numbers and BrdU incorporation suggested that tumor-secreted factors promoted ASC and 3T3-L1 proliferation (Fig. 1*A* and Fig. S1*A*). In contrast, these factors inhibited adipose differentiation of both cell types as indicated by attenuated activity of the lipogenic enzyme glycerol-3-phosphate dehydrogenase (GPDH) (Fig. 1*B*), reduced activation of the key adipogenic transcription factor peroxisome proliferator-activated receptor gamma (PPARγ) (Fig. 1*C*), and inhibition of lipid droplet accumulation (Fig. S1*B*). An experiment in which ASCs and 3T3-L1s were first exposed to TCM and then evaluated for VEGF secretion further suggested that exposure to tumor-derived soluble factors enhances proangiogenic factor release by these cells (Fig. 1*D*). This increased proangiogenic potential is relevant to tumor angiogenesis as tumor-preconditioned ASCs and 3T3-L1s significantly enhanced VEGF-dependent migration of human umbilical vein endothelial cells (HUVECs) as com-

Author contributions: E.M.C., B.R.S., A.Y.N., D.G., C.A.R.-K., and C.F. designed research; E.M.C., B.R.S., J.P.C., R.C.A.E., J.S.L., C.J.Y., D.T.T., J.X.W., L.C., and R.M.W. performed research; L.C., M.R.B., I.C., A.Y.N., and C.A.R.-K. contributed new reagents/analytic tools; E.M.C., B.R.S., J.P.C., R.C.A.E., J.S.L., C.J.Y., D.T.T., J.X.W., S.M., R.M.W., D.G., and C.F. analyzed data; and E.M.C., B.R.S., D.G., and C.F. wrote the paper.

The authors declare no conflict of interest.

*This Direct Submission article had a prearranged editor.

[1]E.M.C. and B.R.S. contributed equally to this work.

[2]To whom correspondence should be addressed. E-mail: cf99@cornell.edu.

This article contains supporting information online at www.pnas.org/lookup/suppl/doi:10.1073/pnas.1121160109/-/DCSupplemental.

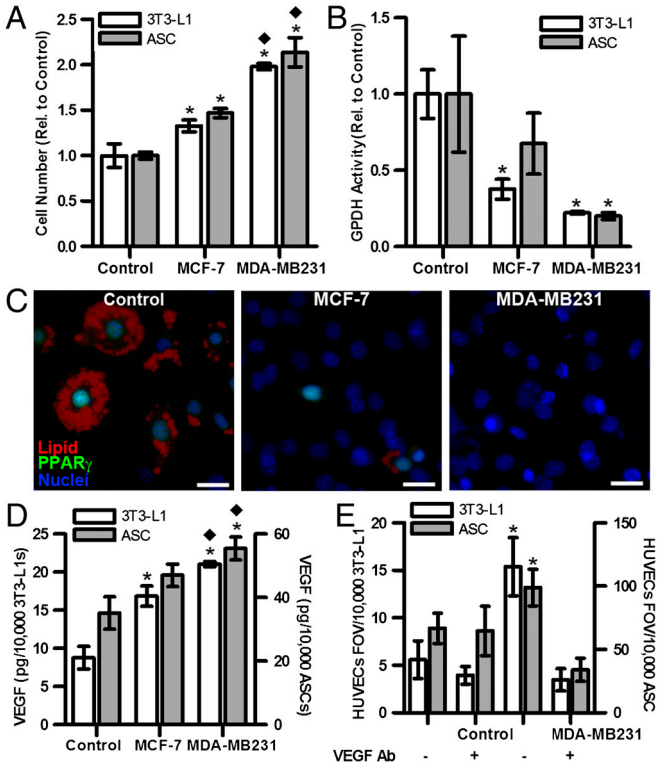

Fig. 1. Tumor-secreted soluble factors regulate ASC function. (*A*) TCM from MCF-7 and MDA-MB231 increases 3T3-L1 and ASC cell numbers relative to control (n = 4). (*B*) TCM treatment significantly decreases the adipogenic capability of 3T3-L1 and ASCs relative to control as determined by spectrophotometric analysis of GPDH activity (n = 4). (*C*) Immunofluorescence analysis of the transcription factor PPARγ in 3T3-L1s confirmed that TCM inhibits adipogenic differentiation. (Scale bar: 20 μm.) (*D*) ELISA suggested that ASCs and 3T3-L1s increase VEGF secretion when preconditioned with TCM from MCF-7 or MDA-MB231 (n = 4). *$P < 0.05$ from control; ◆$P < 0.05$ from MCF-7 condition. (*E*) 3T3-L1s and ASCs that were previously preconditioned with TCM from MDA-MB231 enhanced HUVEC migration in a transwell assay as compared to 3T3-L1s and ASCs preconditioned with control media; addition of a VEGF neutralizing antibody decreased migration to control levels (n = 4). *$P < 0.05$ from all other conditions of the same cell type.

pared to control cells (Fig. 1*E*). Notably, the magnitude of these changes directly correlated with tumor aggressiveness because MDA-MB231-TCM induced greater phenotypic changes than media collected from MCF-7 cultures (Fig. 1 and Fig. S1). Comparison of effects mediated by isogenically matched normal MCF10A, premalignant MCF10AT, and fully malignant MCF10A-CA1a cells confirmed these results. Specifically, premalignant cells had no significant effect on ASC adipogenic differentiation and VEGF secretion but promoted ASC proliferation, whereas MCF10ACA1a cells mediated outcomes similar to MDA-MB231 (Fig. S1 *C–E*). The described observations were broadly relevant as TCM collected from two murine mammary tumor cell lines (16) also enhanced the proliferative and proangiogenic phenotype of adipose progenitor cells and inhibited adipose differentiation (Fig. S2 *A–C*).

To assess whether tumor cells actively recruit ASCs, we performed a transwell migration assay with TCM that revealed that tumor cells attract adipose progenitor cells towards their respective location by enhancing their directed migration (Fig. S2*D*). Collectively, these data suggest that tumor cell-secreted soluble factors enhance the proangiogenic cell population in the tumor stroma by guiding ASC behavior. As TCM similarly modulated ASC and 3T3-L1 behavior, and because data generated with primary cells are typically more robust and generalizable, the studies described in the following experiments were primarily performed with ASCs.

Tumor-Secreted Soluble Factors Enhance ASC Differentiation into ECM-Stiffening Myofibroblasts. Myofibroblasts represent an abundant and proangiogenic cellular component of the tumor stroma whose differentiation is enhanced in the presence of reduced signaling by the adipogenic transcription factor PPARγ (17, 18). Accordingly, ASCs exposed to TCM exhibited increased expression of α-SMA relative to control conditions (Fig. 2*A*), whereby MDA-MB231 exerted a more pronounced effect than MCF-7 (Fig. S3*A*). Next, we evaluated whether tumor cell-derived TGF-β (19), which is pivotal to myofibroblast differentiation and secreted at higher levels by more malignant tumor cells (20), may be involved in inducing phenotypic changes of ASCs. Control media was supplemented with TGF-β at levels found in MDA-MB231-TCM, and this treatment induced ASC differentiation into myofibroblasts as suggested by immunofluorescence and Western Blot analysis (Fig. 2*A* and Fig. S3*B*). Furthermore, addition of a TGF-β epitope-blocking antibody to TCM abrogated myofibroblast differentiation. Whereas these data verify that tumor-secreted TGF-β functions as an upstream mediator of ASC differentiation into myofibroblasts (Fig. 2*A*), other molecules may also play a role. Comparison of control media as well as TCM from MCF-7 and MDA-MB231 via a cytokine antibody array revealed that interleukin-8 (IL-8), VEGF, tumor necrosis factor receptor 1 (TNFR1), and matrix metalloproteinase 3 (MMP3) were enhanced in the TCM (Fig. S3*C*). As IL-8 has been related to myofibroblast differentiation in prostate cancer (21) and was enhanced in MDA-MB231 vs. MCF-7 TCM (Fig. S3*D*), we assessed its effect on ASC myofibroblast differentiation. Results from these studies elucidated that IL-8 regulates ASC differentiation into myofibroblasts in a dose-dependent manner (Fig. S3*E*). These findings are of particular interest as myofibroblasts themselves can upregulate IL-8 (22), which may further promote ASC differentiation into myofibroblasts.

Myofibroblasts mediate tissue stiffening by altering ECM composition and enhancing contraction. In particular, increased collagen I deposition has been associated with increased tumor stiffness and malignancy (23). Our results support that ASC exposure to tumor-derived paracrine signals may contribute to this because ASCs produced significantly more procollagen I (6.0 ± 1.1-fold) and collagen I (4.2 ± 1.1-fold) when treated with TCM rather than control media (Fig. S4). Furthermore, ASCs seeded into microfabricated, free-floating 3D collagen disks differentiated into myofibroblasts, developed stress fibers, and contracted significantly more when cultured in the presence of TCM as compared to control media (Fig. 2 *B* and *C*). These variations in gel contraction were mediated by differences in TCM-mediated changes in myosin-mediated cell contractility rather than proliferation. Specifically, pharmacological inhibitors cytochalasin D (i.e., an agent preventing actin polymerization) or Y-27632 (i.e., an inhibitor of pROCK and thus RhoA signaling) added at levels not affecting cell viability restored the diameter of previously contracted gels (Fig. 2*D*), whereas disks cultured in TCM in the presence of mitomycin C contracted markedly more than similarly treated control disks (Fig. 2*B*). To fully elucidate whether the integrated effects of varied ECM deposition and contraction indeed contribute to enhanced tissue rigidity, the mechanical properties of ASC-seeded disks were analyzed following culture in control or TCM. The shear modulus of these constructs was determined by applying a shear force to one side of a sandwiched gel while measuring the displacement of a photobleached line within the gel (24). Our results indicate that TCM-treated collagen cultures were 1.5-fold stiffer than the control constructs (Fig. 2*E*) confirming the effect of soluble factors on ASC-mediated changes in tissue stiffness. These changes may be explained by varied matrix contraction and irreversible changes in ECM deposition mediated, for example, by increased collagen crosslinking due to enhanced lysyloxidase (LOX) expression by

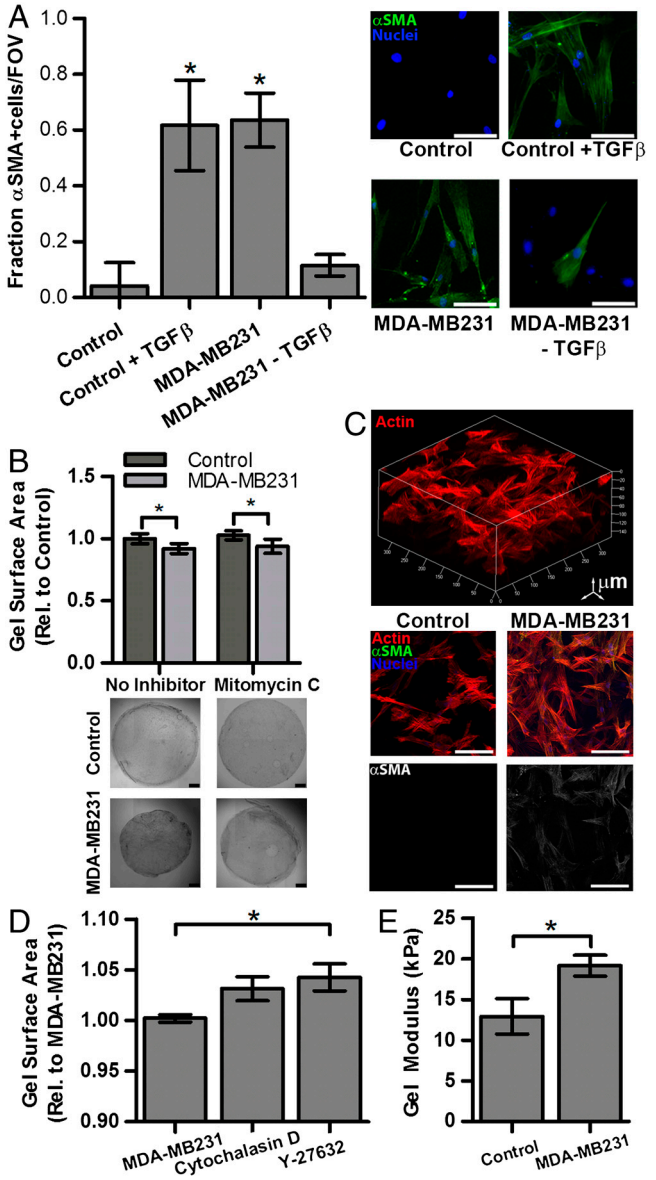

Fig. 2. Tumor-secreted soluble factors enhance ASC differentiation into myofibroblasts. (*A*) Treatment of ASCs with TCM from MDA-MB231 significantly increased the number of α-SMA (green) positive cells as quantified by immunofluorescence image analysis. Addition of TGF-β to control media (control + TGF-β) mimicked this effect, whereas blockade of TGF-β in TCM using a neutralizing antibody (MDA-MB231-TGF-β) inhibited it (n = 4) (Scale bar: 100 μm) *$P < 0.05$ from control and MDA-MB231-TGF-β conditions. (*B*) Collagen gels seeded with ASCs contracted significantly more when cultured in TCM as compared to control medium (n = 6), which occurred even in the presence of the proliferation inhibitor mitomycin C. (Scale bar: 500 μm.) (*C*) Confocal imaging revealed that ASCs within these gels developed stress fibers necessary to generate contractile tension but only differentiated into α-SMA positive cells in the presence of TCM. (Scale bar: 100 μm.) (*D*) Pharmacological inhibition of cytoskeletal tension using cytochalasin D and Y-27632 contributed to the release of the contracted gels as determined via an increase in surface area (n = 3). (*E*) ASC-seeded collagen gels cultured in the presence of TCM were significantly stiffer relative to gels maintained in control media as determined by confocal-based stiffness measurements (n = 5) *$P < 0.05$.

myofibroblasts (25) and/or deposition of additional fibrillar ECM components such as fibronectin (26).

ASCs Respond to ECM Mechanical Properties in a Tumor-Dependent Manner. Normal and tumorigenic cells respond to increased matrix stiffness by adjusting integrin-dependent adhesion, traction forces, and subsequent downstream signaling (10, 27) with effects on cell proliferation and differentiation (28). To test the ability of ASCs to react to tumor-derived and/or self-imposed changes in matrix stiffness we evaluated their adhesion characteristics and corresponding activation of mechanoregulated signaling pathways using hydrogels of pathologically-relevant stiffness (8). Specifically, use of collagen-coated polyacrylamide gels allowed control over mechanical properties of the culture substrates without affecting adhesion ligand density that can independently affect cell behavior (29). ASCs spread significantly more on substrates mimicking breast tumor rigidity (approximately 10 kPa) (8) relative to substrates approximating premalignant (approximately 5 kPa) and adipose tissue (approximately 1 kPa) (8) stiffness (Fig. 3*A*). Traction force microscopy (TFM) confirmed that these morphological changes were accompanied by greater traction forces of ASCs on stiffer relative to more compliant matrices (Fig. 3*A*). These observations directly correlated with the recruitment of phosphorylated focal adhesion kinase (pFAK) to focal adhesions (Fig. 3*B*), a result of activated Rho-ROCK signaling due to force-induced changes in adhesion dynamics (30). Accordingly, ASC number was greater on stiffer matrices, and administration of cytochalasin D and Y-27632 inhibited this effect (Fig. 3*C*) confirming that Rho-ROCK mediated changes in cytoskeletal tension enable ASCs to respond to ECM stiffness.

To assess broadly stiffness-dependent cellular responses to a more relevant, biocompatible material that can be used for adipose tissue engineering and breast reconstruction applications (31, 32), we cultured adipose progenitors on Arg-Gly-Asp (RGD)-modified alginate disks similarly mimicking normal, premalignant, and cancerous breast tissue stiffness. Interestingly, increased stiffness recapitulated the effects of TCM and enhanced cell numbers and VEGF-secretion of these cells while inhibiting their adipogenic differentiation (Fig. S5). These results are consistent with previous studies that indicate elevated adipocyte conversion on more compliant matrices (28, 33) and with less spread, rounder cell morphology (34).

To investigate whether tumor-secreted soluble factors enhance ASC response to ECM rigidity, ASCs were cultured on polyacrylamide substrates of a broad range of stiffnesses (0.2–30 kPa) in the presence or absence of TCM from MCF-7 or MDA-MB231. Cell growth was commensurate with increasing stiffness, whereas the level of tumor malignancy affected ASC stiffness response. More specifically, TCM from the more malignant MDA-MB231 cells increased cell growth on gels of lower stiffness relative to TCM of the less malignant MCF-7 (Fig. 3*D*). Furthermore, the combined effects of ECM stiffness and tumor-derived soluble factors promoted cellular alignment on stiffer (but not soft) matrices, and this effect was more pronounced with TCM from MDA-MB231 than MCF-7 (Fig. 3*E*). Collectively, these results suggest that tumor-secreted factors dramatically enhance adipose-derived stem cell responses to stiffness leading to (*i*) an increased contractile cell population and (*ii*) directed force generation (35) that may ultimately exacerbate tumor rigidity and hence malignancy.

ASCs Modulate Tumor Progression In Vivo. To determine the relevance of our in vitro findings to tumor growth in vivo, ASCs and MDA-MB231 cells were injected individually or in combination into the cleared mammary fat pad of immunocompromised mice. Coinjection of MDA-MB231 with ASCs yielded larger tumors than delivery of tumor cells alone in accordance with previous results (36, 37) (Fig. 4*A*). In contrast, injected ASCs largely formed adipose tissue (Fig. 4*C*) that was similar in size to explants from sham-injected media suggesting that the difference in tumor size was caused by varied tumor malignancy rather than the additional volume assumed by the coinjected ASCs (Fig. 4*A*). Furthermore, tumors resulting from the mixture of ASCs and MDA-MB231 cells appeared more locally invasive upon explan-

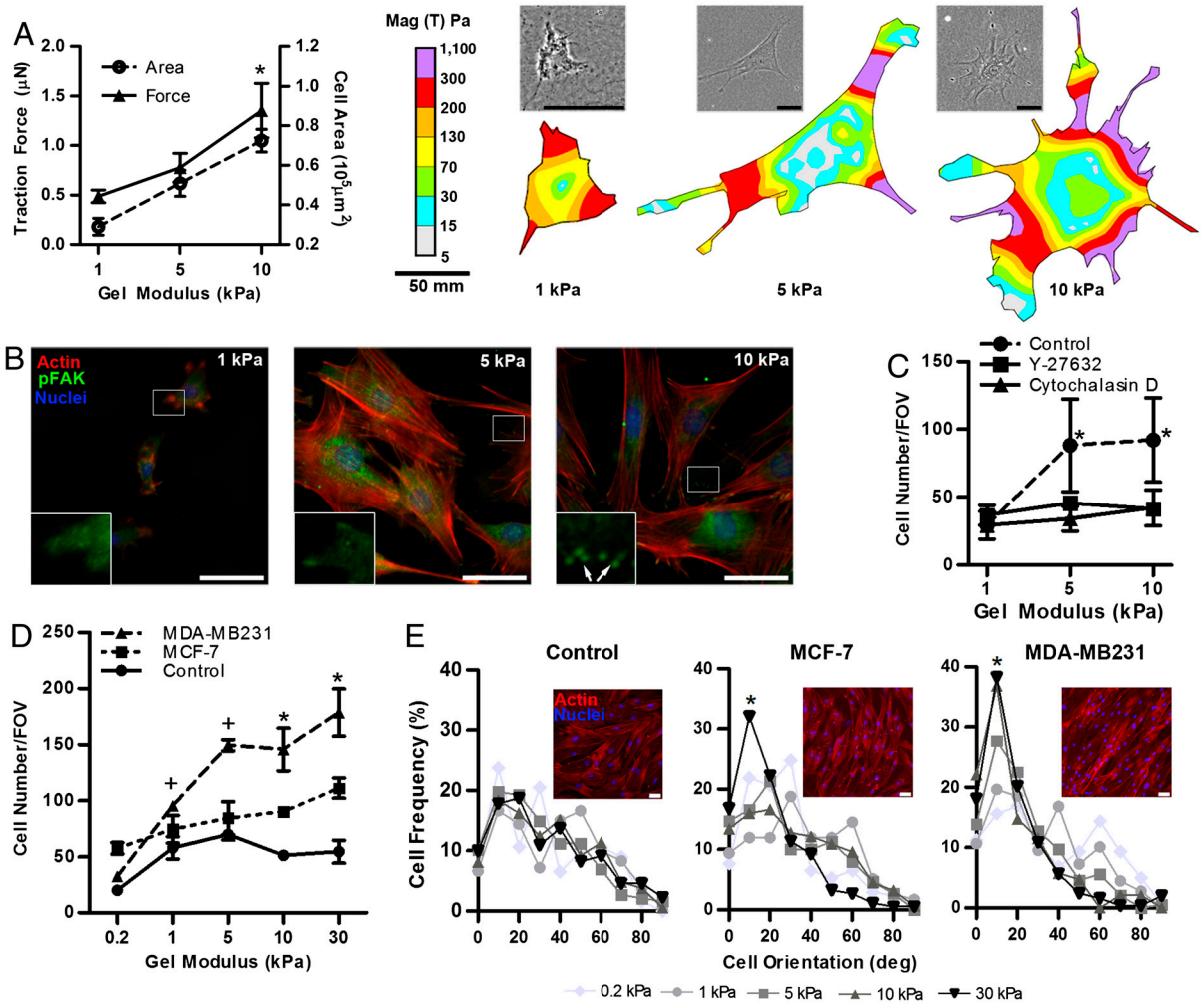

Fig. 3. ASC response to matrix mechanical properties. (*A*) TFM indicated that ASCs cultured on hydrogels of increased stiffness spread significantly more and exert greater traction forces relative to cells cultured on soft matrices; representative ASC phase images with corresponding traction maps are shown (n = 13–32, error bars represent standard errors) (Scale bar: 50 μm) *$P < 0.05$ from 1 kPa condition. (*B*) Immunofluorescence indicates increased recruitment of pFAK[Y397] to ASC focal adhesions on stiffer matrices (white arrows). (Scale bar: 20 μm.) (*C*) Cell counting suggested that increased matrix stiffness enhances ASC numbers and that pharmacological inhibition of cytoskeletal tension with Y-27632 or cytochalasin D inhibits this effect (n = 4). (*D*) ASC numbers on stiff matrices were further enhanced with culture in TCM whereby TCM from MDA-MB231 exerted a more pronounced effect than TCM from MCF-7 (n = 3) *$P < 0.05$ between all conditions; +$P < 0.05$ between MDA-MB231 and control conditions. (*E*) Image analysis of the deviation from the average angle of phalloidin-stained cells revealed that ASC alignment represented an integrated effect of substrate stiffness and tumor malignancy, whereas ASCs on 30 kPa gels had enhanced alignment in MCF-7 TCM. This occurred on gels of even lower stiffness in MDA-MB231 TCM *$P < 0.05$. (Scale bar: 50 μm.)

tation relative to MDA-MB231-borne tumors that were easily demarcated for dissection. Pathological evaluation of H&E-stained cross-sections confirmed this assessment and revealed an enhanced degree of local invasion and desmoplasia for the coimplanted tumors vs. the control tumors (Fig. S6 *A* and *B*). Additionally, cytological features of malignancy (multinucleated cells and rosettes) were augmented in the coimplanted group as compared to the MDA-MB231 group (Fig. S6*C*). To correlate variations in tumor growth with differences in myofibroblast differentiation, immunohistochemical analysis was performed that confirmed that the density of α-SMA myofibroblastic cells (Fig. 4*B*) was increased in tumors originating from coinjection of both cell types rather than tumor cells alone. Circulating ASCs can be recruited to and associate with blood vessels in the form of α-SMA pericytes (38). In our coimplantation studies, however, immunohistochemical analysis of desmin, a pericyte marker (39), verified that the majority of α-SMA positive cells were myofibroblasts rather than pericytes as desmin staining showed no significant difference ($p = 0.33$) between coimplanted and control tumors. Nevertheless, blood vessel density was greater in the coimplantation group (Fig. 4*C*), and ELISA of tumor lysates suggested that ASC/myofibroblast secretion of proangiogenic VEGF and IL-8 (12, 22) may have contributed to these differences (Fig. S7).

To evaluate if varied myofibroblast content correlated with increased stiffness, we determined the mechanical properties of the different tumors via Dynamic Mechanical Thermal Analysis (DMTA) compression tests on tumor sections in the elastic regime of deformation. The mean Young's modulus (E) was more than 50% higher in tumors generated by coimplantation of ASCs than in those generated in the absence of ASCs (3.1 ± 1.2 kPa vs. 2.0 ± 0.8 kPa, $P < 0.04$) (Fig. 4*D* and Fig. S8). Data from the full elastic and plastic regime of deformation (Fig. S8*B*) additionally indicated that tumors from the coimplanted group exhibit higher stiffness and a smaller range of elastic (reversible) deformation than tumors grown without ASCs. Consistent with these results, tumors resulting from coinjection contained more procollagen I and collagen (Fig. S9 *A* and *B*), were characterized by enhanced collagen fibril maturity and linearity (Fig. S9 *C* and *D*), and likely also comprised increased fibronectin (26). Such changes are indicative of enhanced desmoplasia and aggressiveness (23) and may further contribute to ASC-mediated changes in tumor

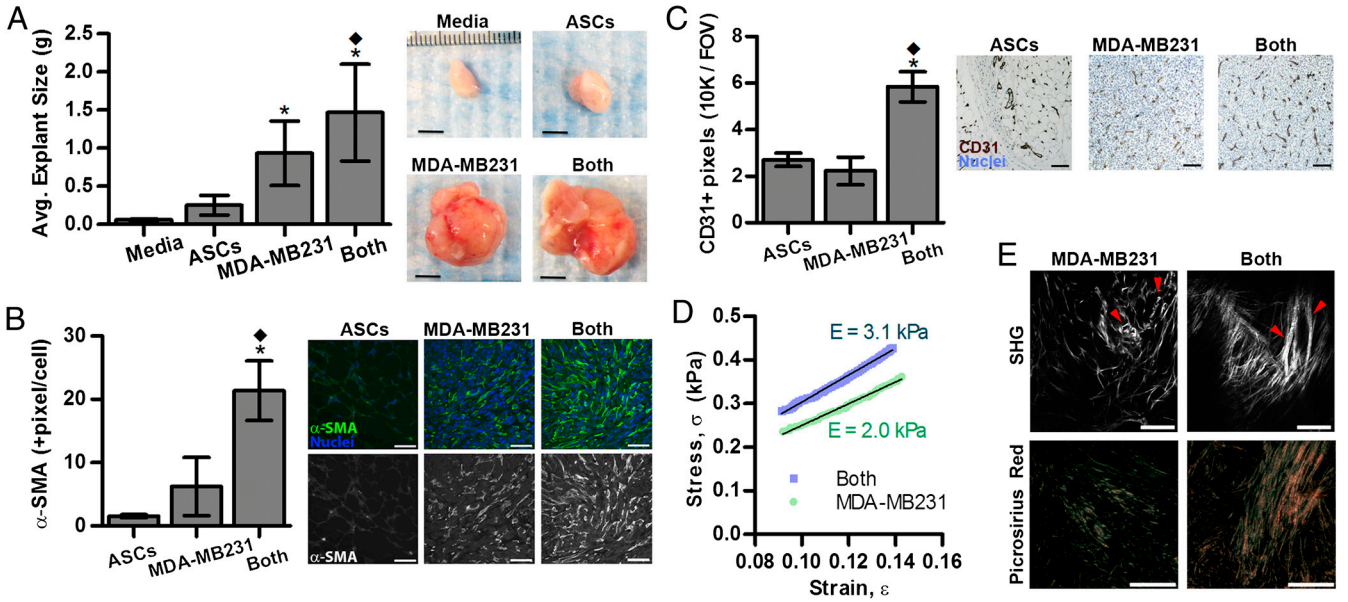

Fig. 4. ASCs modulate tumor progression in vivo. (*A*) Tumors resulting from the coinjection of ASCs and MDA-MB231 cells (both) (n = 14) were significantly larger than tumors formed by MDA-MB231 cells alone (n = 16). Soft tissue explants generated from injected ASCs (n = 12) or media (n = 2) are shown for a comparison. (Scale bar: 5 mm.) (*B*) Immunofluorescence analysis indicates that α-SMA levels were greatest in the explants resulting from coimplantation of ASCs and MDA-MB231 cells as compared to those from MDA-MB231 and ASCs alone. (Scale bar: 50 μm.) (*C*) Similarly, the density of CD31+ blood vessels was enhanced in explants from the coimplanted group. (Scale bar: 20 μm.) For α-SMA and CD31+ image analysis, ASC (n = 6) (both) (n = 6), and MDA-MB231 (n = 12) explants were analyzed. (*D*) Mechanical analysis of tumor sections via DMTA. The mean stress-strain profile was measured in PBS at room temperature through the low-strain (9–14%) elastic regime. The engineering stress σ vs. strain ε curve represents the average of two compressions per tumor section performed on four tumor sections from MDA-MB231 alone and nine tumor sections from the coimplantation group (see *SI Materials and Methods*.). The mean Young's modulus (*E*) was extracted from the slope of the stress-strain curve, $\sigma = E\varepsilon$. (*E*) Compared to tumors from MDA-MB231, coinjected tumors contain more mature and linearized collagen fibers as revealed by picrosirius red staining of cross-sections and second harmonic generation (SHG) imaging (Scale bar: 100 μm), which is further quantified in Fig. S9. For (*A–C*) *$P < 0.05$ from ASCs condition; ◆$P < 0.05$ from MDA-MB231 condition.

growth; decellularized matrices of TCM-preconditioned adipose progenitors increased tumor cell growth relative to matrices from control cells in a manner dependent on generation of cytoskeletal tension (Fig. S9*E*). Nevertheless, additional conditions including paracrine signaling between ASC-derived cells and tumor cells may also contribute to the observed changes in tumor growth in our studies (36).

Conclusions

Breast cancer cell signaling may undermine normal ASC function to form a physicochemical microenvironment that promotes tumorigenesis. Epidemiologically, controversy still exists as to whether fat grafting procedures contribute to recurrence of breast cancer (40). Our findings suggest this possibility and long-term follow up studies will be needed in which not only the use of "simple" fat, but implants concentrated with ASCs are evaluated. Additionally, the results presented herein provide a possible explanation for why obesity-associated with an increased pool of ASCs-represents a risk factor for breast cancer (41, 42) and highlight novel design parameters for ASC-based breast reconstruction. Specifically, ASCs are frequently applied using relatively rigid biomaterial scaffolds or hydrogels (43, 44), but vehicles mimicking the mechanical properties of adipose tissue and potentially codelivery of morphogens are needed to ensure adipose tissue functionality. In particular, PPARγ agonists may represent attractive candidate molecules due to their ability to promote adipogenesis while inhibiting myofibroblast differentiation (18). Determination of whether tumor-related changes of ASC functions are due to selective mechanisms or cell fate instruction will also be needed to help increase the safety of such applications. Although the goal of the present study was to better define the physicochemical contributions of ASCs to breast cancer, a variety of other cancers may also depend on such phenomena. Because ASCs can be activated and released into the circulation to participate in tumor progression at spatially distinct sites, they may, for example, impair the prognosis of prostate (45) and colorectal cancer patients (46). Collectively, therapeutic application of ASCs independent of site should be carefully considered in patients previously treated for cancer, and the use of cell delivery vehicles accurately mimicking nontumorigenic microenvironmental conditions should be a prerequisite.

Materials and Methods

Cell Culture. 3T3-L1, MDA-MB231, MCF-7 (all from ATCC), and MCN1 and MCN2 mammary tumor cells isolated from the mammary epithelium of MMTV-Cre, $p53^{L/L}$, MMTV-Cre, and $p53^{L/L}$ $Rb^{L/L}$, respectively (16), were routinely cultured in MEM (α-modification (αMEM) (Sigma) containing 10% FBS (Tissue Culture Biologicals) and 1% antibiotic (penicillin/streptomycin, Gibco). MCF-10A (ATCC), MCF10AT1, and MCF10ACA1a (both from Barbara Ann Karmanos Cancer Institute) (47) were maintained in DMEM/F12 supplemented with horse serum, epidermal growth factor (EGF), hydrocortisone, cholera toxin, insulin, and penicillin/streptomycin (all from Invitrogen) (48). ASCs and HUVECs (both from Lonza) were cultured in their corresponding growth media (ADSC-GM and EGM-2, respectively; Lonza). Lonza isolates ASCs from lipoaspirates based on expression of stem cell-associated surface markers (49), cryopreserves cells at passage one, and does not pool cells from multiple sources. Here, ASCs from two separate female donors were utilized at passages less than seven. ASC function in response to TCM and matrix mechanical properties was assessed (see *SI Materials and Methods*). Additionally, the effect of 3T3-L1-derived matrices on MDA-MB231 cell growth was measured (see *SI Materials and Methods*).

In Vivo Studies. Media, ASCs and/or MDA-MB231 cells ($1 \cdot 10^6$ in 20 μL of DMEM/ Ham's F-12, 10% FBS, 1% antibiotic) were injected into the cleared mammary fat pad of at least six three- week-old female SCID/NCr mice (Charles River Labs, 01S11) (two tumors per mouse) per condition in accordance with Cornell University animal care guidelines. Explants were harvested six weeks after implantation, imaged, weighed, and divided for subsequent formalin-fixation/paraffin-embedding and lysis in T-PER buffer (Pierce). H&E-stained sections were broadly evaluated for pathological features of malignancy. Cross-sections were characterized further via immunohistochemical

staining for CD31, α-SMA, procollagen I, and desmin, whereas collagen was stained via Masson's Trichrome. For staining procedures and image analysis methods, see *SI Materials and Methods*. VEGF and IL-8 content in lysates was measured via VEGF and IL-8 DuoSets (R&D Systems) and normalized to protein content as determined via bicinchoninic acid protein assay (Thermo Scientific). Tumor stiffness was determined using a DMTA as further outlined in *SI Materials and Methods*.

Statistical Analysis. Statistical analysis was performed using GraphPad Prism 5. Student's *t* tests were used to compare two data sets, whereas ANOVA was applied to determine the statistical significance of the differences between data sets of three or more using the Tukey method to make post-hoc pairwise comparisons. A p-value less than 0.05 was considered statistically significant. Data are represented as average ± standard deviations with the exception of the traction force measurements that are shown with standard errors.

ACKNOWLEDGMENTS. Dr. David Infanger for aid in manuscript preparation, Kerstin Höger, Ana Martin-Ryals, and Christina Cossell for experimental aid, and Andrea Flesken-Nikitin for help with animal experiments. Funding by NIH/NCI RC1 CA146065 (to C.F.), R21 CA161532 (to C.F. and D.G.), R01 CA96823 (to A.Y.N.), the Cornell Center on the Microenvironment and Metastasis through Award Number NCI U54 CA143876 (to C.F., C.R.K., I.C., and R.M.W.), NSF CMMI-1031068 (to D.G.), and Graduate Research Fellowship (to E.M.C.). The content is solely the responsibility of the authors and does not necessarily represent the official views of NCI or NIH.

1. Cherubino M, Marra KG (2009) Adipose-derived stem cells for soft tissue reconstruction. *Regen Med* 4:109–117.
2. Gimble JM, Katz AJ, Bunnell BA (2007) Adipose-derived stem cells for regenerative medicine. *Circ Res* 100:1249–1260.
3. Surgeons ASoP (2010) Report of the 2010 Plastic Surgery Statistics: ASPS National Clearinghouse of Plastic Surgery Procedural Statistics., Available at www.plasticsurgery.org.
4. Moioli EK, et al. (2010) Hybrid adipogenic implants from adipose stem cells for soft tissue reconstruction in vivo. *Tissue Eng Part A* 16:3299–3307.
5. Yoshimura K, et al. (2008) Cell-assisted lipotransfer for cosmetic breast augmentation: Supportive use of adipose-derived stem/stromal cells. *Aesthetic Plast Surg* 32:48–55 discussion 46–47.
6. Brewster AM, et al. (2008) Residual risk of breast cancer recurrence five years after adjuvant therapy. *J Natl Cancer Inst* 100:1179–1183.
7. Janmey PA, Levental I, Georges PC (2007) Soft biological materials and their impact on cell function. *Soft Matter* 3:299–306.
8. Samani A, Bishop J, Luginbuhl C, Plewes DB (2003) Measuring the elastic modulus of ex vivo small tissue samples. *Phys Med Biol* 48:2183–2198.
9. Butcher DT, Alliston T, Weaver VM (2009) A tense situation: Forcing tumour progression. *Nat Rev Cancer* 9:108–122.
10. Paszek MJ, et al. (2005) Tensional homeostasis and the malignant phenotype. *Cancer Cell* 8:241–254.
11. Mammoto A, et al. (2009) A mechanosensitive transcriptional mechanism that controls angiogenesis. *Nature* 457:1103–1108.
12. Nakagawa H, et al. (2004) Role of cancer-associated stromal fibroblasts in metastatic colon cancer to the liver and their expression profiles. *Oncogene* 23:7366–7377.
13. Kidd S, et al. (2012) Origins of the tumor microenvironment: Quantitative assessment of adipose-derived and bone marrow-derived stroma. *PLoS One* 7:e30563.
14. Quante M, et al. (2011) Bone marrow-derived myofibroblasts contribute to the mesenchymal stem cell niche and promote tumor growth. *Cancer Cell* 19:257–272.
15. Cornelius P, MacDougald OA, Lane MD (1994) Regulation of adipocyte development. *Annu Rev Nutr* 14:99–129.
16. Cheng L, et al. (2010) Rb inactivation accelerates neoplastic growth and substitutes for recurrent amplification of cIAP1, cIAP2 and Yap1 in sporadic mammary carcinoma associated with p53 deficiency. *Oncogene* 29:5700–5711.
17. Olaso E, et al. (2003) Proangiogenic role of tumor-activated hepatic stellate cells in experimental melanoma metastasis. *Hepatology* 37:674–685.
18. Hong KM, Belperio JA, Keane MP, Burdick MD, Strieter RM (2007) Differentiation of human circulating fibrocytes as mediated by transforming growth factor-beta and peroxisome proliferator-activated receptor gamma. *J Biol Chem* 282:22910–22920.
19. De Wever O, Mareel M (2003) Role of tissue stroma in cancer cell invasion. *J Pathol* 200:429–447.
20. Guerrero J, et al. (2010) Soluble factors derived from tumor mammary cell lines induce a stromal mammary adipose reversion in human and mice adipose cells. Possible role of TGF-beta1 and TNF-alpha. *Breast Cancer Res Treat* 119:497–508.
21. Schauer IG, Ressler SJ, Tuxhorn JA, Dang TD, Rowley DR (2008) Elevated epithelial expression of interleukin-8 correlates with myofibroblast reactive stroma in benign prostatic hyperplasia. *Urology* 72:205–213.
22. Yagi Y, Andoh A, Inatomi O, Tsujikawa T, Fujiyama Y (2007) Inflammatory responses induced by interleukin-17 family members in human colonic subepithelial myofibroblasts. *J Gastroenterol* 42:746–753.
23. Levental KR, et al. (2009) Matrix crosslinking forces tumor progression by enhancing integrin signaling. *Cell* 139:891–906.
24. Buckley MR, Bergou AJ, Fouchard J, Bonassar LJ, Cohen I (2010) High-resolution spatial mapping of shear properties in cartilage. *J Biomech* 43:796–800.
25. Peyrol S, et al. (1997) Lysyl oxidase gene expression in the stromal reaction to in situ and invasive ductal breast carcinoma. *Am J Pathol* 150:497–507.
26. Chandler EM, Saunders MP, Yoon CJ, Gourdon D, Fischbach C (2011) Adipose progenitor cells increase fibronectin matrix strain and unfolding in breast tumors. *Phys Biol* 8:015008.
27. Reinhart-King CA, Dembo M, Hammer DA (2003) Endothelial cell traction forces on RGD-derivatized polyacrylamide substrata. *Langmuir* 19:1573–1579.
28. Engler AJ, Sen S, Sweeney HL, Discher DE (2006) Matrix elasticity directs stem cell lineage specification. *Cell* 126:677–689.
29. Shin H, Zygourakis K, Farach-Carson MC, Yaszemski MJ, Mikos AG (2004) Modulation of differentiation and mineralization of marrow stromal cells cultured on biomimetic hydrogels modified with Arg-Gly-Asp containing peptides. *J Biomed Mater Res A* 69:535–543.
30. McLean GW, et al. (2005) The role of focal-adhesion kinase in cancer—A new therapeutic opportunity. *Nat Rev Cancer* 5:505–515.
31. Cho SW, et al. (2005) Engineering of volume-stable adipose tissues. *Biomaterials* 26:3577–3585.
32. Davidenko N, Campbell JJ, Thian ES, Watson CJ, Cameron RE (2010) Collagen-hyaluronic acid scaffolds for adipose tissue engineering. *Acta Biomater* 6:3957–3968.
33. Chandler EM, et al. (2011) Stiffness of photocrosslinked RGD-alginate gels regulates adipose progenitor cell behavior. *Biotechnol Bioeng* 108:1683–1692.
34. McBeath R, Pirone DM, Nelson CM, Bhadriraju K, Chen CS (2004) Cell shape, cytoskeletal tension, and RhoA regulate stem cell lineage commitment. *Dev Cell* 6:483–495.
35. Storm C, Pastore JJ, MacKintosh FC, Lubensky TC, Janmey PA (2005) Nonlinear elasticity in biological gels. *Nature* 435:191–194.
36. Muehlberg FL, et al. (2009) Tissue-resident stem cells promote breast cancer growth and metastasis. *Carcinogenesis* 30:589–597.
37. Prantl L, et al. (2010) Adipose tissue-derived stem cells promote prostate tumor growth. *Prostate* 70:1709–1715.
38. Zhang Y, et al. (2009) White adipose tissue cells are recruited by experimental tumors and promote cancer progression in mouse models. *Cancer Res* 69:5259–5266.
39. Kida Y, Duffield JS (2011) Pivotal role of pericytes in kidney fibrosis. *Clin Exp Pharmacol Physiol* 38:417–423.
40. Petit JY, et al. (2011) Locoregional recurrence risk after lipofilling in breast cancer patients. *Ann Oncol* 23:582–588.
41. van Harmelen V, et al. (2003) Effect of BMI and age on adipose tissue cellularity and differentiation capacity in women. *Int J Obes Relat Metab Disord* 27:889–895.
42. Bianchini F, Kaaks R, Vainio H (2002) Overweight, obesity, and cancer risk. *Lancet Oncol* 3:565–574.
43. Moutos FT, Guilak F (2010) Functional properties of cell-seeded three-dimensionally woven poly(epsilon-caprolactone) scaffolds for cartilage tissue engineering. *Tissue Eng Part A* 16:1291–1301.
44. Ochoa I, et al. (2011) Mechanical properties of cross-linked collagen meshes after human adipose derived stromal cells seeding. *J Biomed Mater Res A* 96:341–348.
45. Lin G, et al. (2010) Effects of transplantation of adipose tissue-derived stem cells on prostate tumor. *Prostate* 70:1066–1073.
46. Bellows CF, Zhang Y, Chen J, Frazier ML, Kolonin MG (2011) Circulation of progenitor cells in obese and lean colorectal cancer patients. *Cancer Epidemiol Biomarkers Prev* 20:2461–2468.
47. Santner SJ, et al. (2001) Malignant MCF10CA1 cell lines derived from premalignant human breast epithelial MCF10AT cells. *Breast Cancer Res Treat* 65:101–110.
48. Kraning-Rush CM, Califano JP, Reinhart-King CA (2012) Cellular traction stresses increase with increasing metastatic potential. *PLoS One* 7:e32572.
49. Lonza (2011) Poietics™ human adipose derived stem cells (ADSC)., Doc INST PT-5006-4, available at www.lonza.com.